Nano Energy 110 (2023) 108310

Contents lists available at ScienceDirect

Nano Energy

journal homepage: www.elsevier.com/locate/nanoen

Grounding strategy to promote the surface charge equilibrium and output performance of triboelectric nanogenerator

Jingyi Jiao [a], Jinmei Liu [a], Long Gu [a], Nuanyang Cui [a,*], Yong Qin [b,*]

[a] School of Advanced Materials and Nanotechnology, Xidian University, Xi'an 710071, China
[b] Institute of Nanoscience and Nanotechnology, School of Materials and Energy, Lanzhou University, Gansu 730000, China

ARTICLE INFO

Keywords:
TENG
Grounding strategy
Surface charge density
Output power
Charge quantity per cycle (CQC)

ABSTRACT

As the driving force for the flow of electrons in the external circuit, the quantity of triboelectric charges in the friction layers is critical important, more triboelectric charges will bring about the larger output power of a triboelectric nanogenerator (TENG). In this work, a grounding strategy is proposed and developed to further increase the triboelectric charge density of the friction layer and the output of TENG, which can break through the limitations of increasing the output of TENG by merely enhancing material's property itself. By designing the external circuit and utilizing an additional ground electrode, the electrons in the electron donor layer can be replenished timely, which contributes to a 2 times improvement in output current and 10 times improvement in output power. Additionally, the grounding strategy is used to improve the performance of sound wave-driven TENG (STNG). We found that the improvement effect of the grounding strategy on STNG's (GS-enhanced STNG) output increases with the increasing of sound frequency, and the output power of this GS-enhanced STNG can be increased by 200 times.

1. Introduction

With the development of portable and mobile electronic equipment, more and more energy sources have been explored to power these kinds of widely and dispersively distributed electronic devices. The emergence of triboelectric nanogenerators [1–3] (TENGs) provides new a power source, it is an energy harvester which based on the coupling effect of triboelectrification and electrostatic induction. It can convert various forms of micro-mechanical energy from the environment into electricity at any time, also, it has the merits of lower production costs, higher energy-conversion efficiency and wider range selection of materials [4, 5]. Since it was invented, the ways of increasing the output performance has always been the core problem for TENG. Based on its working mechanism, the maximum amount of charges that can be stored or generated on the friction layer determines the threshold value of a TENG's output charges per half cycle. Under the same driving conditions, TENG with higher surface charge density will produce much greater output performance. At present, the low surface charge density of friction layers leads to the unstable and relatively low electrical output, which largely limits TENG's real applications. So, exploring the effective methods for enhancing the surface charge density [6–8] of friction layers and output power of TENGs is quite important in this research field.

In general, the surface charge density of TENG's friction layers is simultaneously confined by some factors such as triboelectric charging, air breakdown and dielectric breakdown, which can be described by the formula 1 [9–12].

$$\sigma_{TENG} = min\left(\sigma_{triboelectrification}, \sigma_{dielectricbreakdown}, \sigma_{airbreakdown}\right) \quad (1)$$

Therein,σ_{TENG} represents the charge density of the friction layer of this TENG, $\sigma_{triboelectrification}$ represents the surface charge density generated by triboelectrification, $\sigma_{dielectric\ breakdown}$ represents the maximum charge density that the dielectric layer can store [13], and $\sigma_{airbreakdown}$ represents the residual surface charge density after air breakdown [14]. During the working process of the TENG [15], the growth trend of surface charges which generated by triboelectrification is from fast to slow and finally remains steady. Meanwhile, as the charges accumulate, some of the surface charges would lose at the same time due to the existence of the leakage current and the air breakdown effect [16]. These unavoidable charge losses and the limited surface charges generated by triboelectrification will make the surface charge density [17–19] of the TENG reach to a certain equilibrium value instead of constantly increasing. In

* Corresponding authors.
E-mail addresses: nycui@xidian.edu.cn (N. Cui), qinyong@lzu.edu.cn (Y. Qin).

https://doi.org/10.1016/j.nanoen.2023.108310
Received 22 December 2022; Received in revised form 24 February 2023; Accepted 26 February 2023
Available online 28 February 2023

fact, the previous reported works have proved that the effective ways to increase the charge density of friction layers is to break the original equilibrium state and to re-establish a new equilibrium.

Usually, the strategies to improve the surface charge density of the friction layer are usually as follows: surface modification of materials [20], selection of materials with more appropriate dielectric constant [21] or large difference in electronegativity [22,23], controlling the experimental environment [24,25], adding lubricants [26–28], adding ferroelectric polymer films [29], designing alternating magnetic stripe arrays [30], designing shielding layer and alternative blank-tribo-area [31] and so on. For the methods of surface modification of materials, many methods including construction of surface microstructure, chemical surface functionalization or surface ion implantation have been developed [12,32,33]. As for the strategy of selecting material with suitable dielectric constant, the maximum charge density of the dielectric layer is related to its dielectric constant. According to Gauss theorem [34], the larger the dielectric constant, the smaller the electric field intensity, and electric field force would also become smaller to drive the flown electrons. As a result, the charge loss rate would be slow down and the surface charge density would decrease more slowly [9,35,36]. For the selection of electronegativity, the materials with large electronegativity differences possess different charge inflow rates, permittivity, and conductivity, which will lead to various charge loss rates. So, choosing materials with different electronegativity is a comprehensive factor for the researchers to consider. Except the above strategies, it is important to investigate the strategies which can establish a new equilibrium of the surface charge of TENGs [11,37–39]. Based on the above discussions and the working mechanism of TENG, it can be put forward that as the friction charges are transferred, the friction layer with strong electronegativity between two friction layers will lose electrons and be positive. The absence of electrons would prevent the further separation of new friction charges, so that the separation rate of friction charges will be reduced. Taking that into consideration, we think that if the electrons in the electron donor layer can be replenished from the ground, which will break the original equilibrium of charge separation, and a new equilibrium would be established, more triboelectric charges would distribute in two friction layers, which will contribute to the enhancement of TENG's output.

So, in this work, a grounding strategy is proposed and developed to enhance the output of TENG. After further optimizations, the output current of grounding strategy enhanced TENG (GTNG) reaches 0.12 μA/cm^2 and the output power is 45 μW/cm$^{2,\ \text{which are}}$ 2 times and 10 times the value of the normal TENG without grounding strategy respectively. Meanwhile, we also observed the one-way net inflow of the electrons in the electron donor layer through the grounding wire. This phenomenon proves that the enhancement effect of grounding strategy on the TENG's output performance. To further check the effectiveness and applicability of grounding strategy, we attempted to enhance the output of a sound wave-driven triboelectric nanogenerator (STNG) using this strategy. The output power of grounding strategy enhanced STNG increases nearly 200 times comparing with the normal STNG without utilizing the grounding strategy.

1.1. The enhancement effect of grounding strategy on TENG's output performance

The schematic diagram of the grounding strategy enhanced TENG (GTNG) and its electric field distribution are shown in Fig. 1**a**, and its picture of actual working state is displayed in Supplementary Fig. 1. There are two major parts in this device: the upper part is a copper-paper-copper structure, the outer copper (Cu) acts as the electrode, the inner Cu acts as the positive friction layer; the lower part is a FEP-Cu double layer structure, with Cu as the electrode and FEP as the negative friction layer. The outer Cu electrode in the upper part is connected to the earth through a conducting wire, and the dielectric layer thickness of 15 μm. In this experiment, the reasons for choosing FEP as the negative friction layer are explained in the Supplementary Note 1 in detail, and the relevant comparison and validation tests are shown in the Supplementary Fig. 2 and 3. For a general TENG, during its working process, the output voltage and output current tends to increase gradually and then keep stable. This is because that the friction charges gradually accumulates in the friction layer, and reaches an upper limit maximum

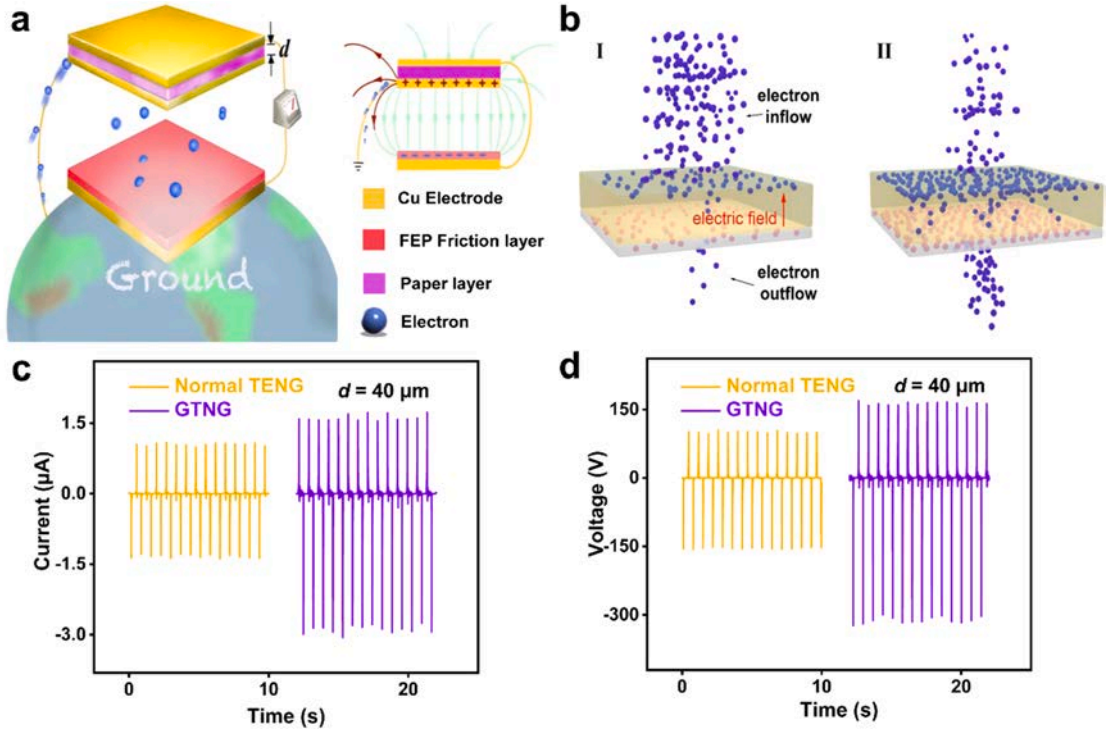

Fig. 1. (a) The schematic and electric field distribution diagram of GTNG with dielectric layer. (b)The surface charge equilibrium process of a friction layer. (c-d) Comparison of output current and voltage signals of the normal TENG and the GTNG.

under the driving process. Actually, the existence of the upper limit reflects there is a dynamic equilibrium state of the friction electrons on the friction layer, Fig. 1**b** depicts the overall process of this dynamic equilibrium. At the initial state, the negative friction layer plundered electrons from the opposite positive friction layer, and making electrons accumulate on its surface. At the same time, owing to the induced positive charges on the electrode behind the negative friction layer, the internal electric field in this friction layer is generated. Under the action of this electric field, part of the electrons accumulated on the surface of the friction layer will flow to the back electrode, resulting in the loss of electrons on the surface. As the charge accumulates, the inflow of electrons of the TENG would gradually decrease, and the outflow of electrons of the TENG will gradually increase, then the frictional electrons will reach a dynamic equilibrium state. Correspondingly, the output voltage and output current of the TENG would reach a stable state. If we want to increase the surface charge density of the friction layer for increasing the output performance of the TENG, we need to break the original dynamic equilibrium state of electrons in the friction

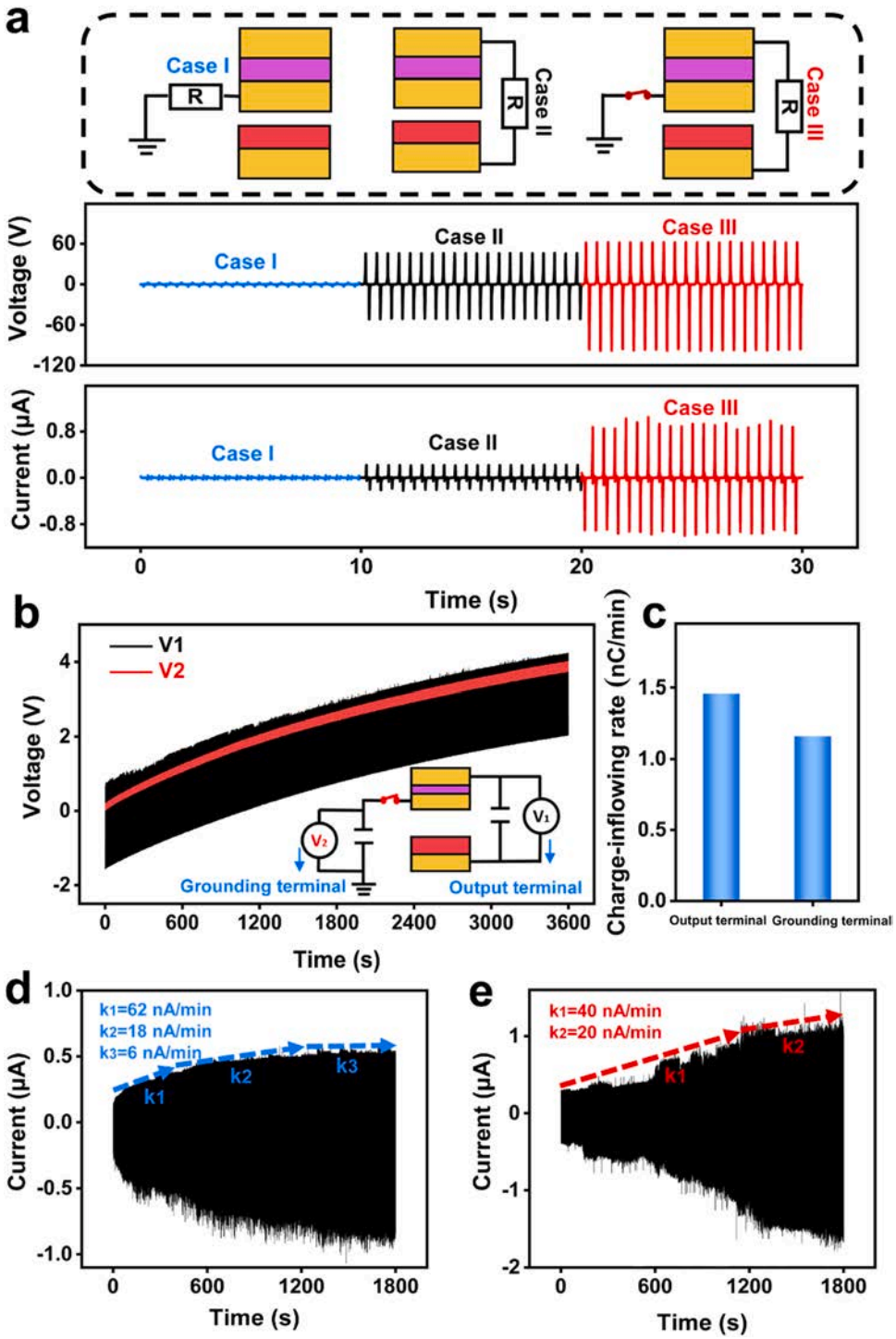

Fig. 2. (a) External circuit diagram and the comparison of electrical signal in three cases (b) Testify and comparison of the electrons inflowing from the earth and that inside the GTNG. (c) Comparison of the charge-inflowing rate of the mentioned two states. (d)Without grounding strategy, the current variation curve of normal TENG. (e) Adopting grounding strategy, the current variation curve of GTNG.

layer and increase its maximum charge carrying capacity of electrons by means of improving the inflow of electrons or decreasing the outflow of electrons.

In this work, an electron flowing channel between the friction layer and the earth is constructed by grounding the positive friction layer (the inner Cu layer of nanogenerator's upper part). When the positive friction layer is positively charged due to the loss of electrons, the electric field scattered outside its edge will pull the electrons in the earth into the friction layer, which can make the GTNG generate more separated friction charges, and increase the flowing rate of friction electrons into the negative friction layer in the lower part of GTNG. This would break the original dynamic equilibrium state of electrons, move more friction electrons into the negative friction layer to reach a new dynamic equilibrium state of electrons with larger surface charge density on friction layer, then increase the output performance of TENG. Experimentally, it is found that the output performance of GTNG is obviously improved comparing with the general TENG without using this grounding strategy. As shown in Fig. 1**c and d**, under the same driving conditions, the open-circuit voltage and short-circuit current of the comparison device (general TENG without grounding strategy, dielectric layer thickness of 15 μm) are about 150 V and 1.5 μA, respectively. The open circuit voltage and short circuit current of GTNG with same dielectric layer thickness are increased to about 300 V and 3.0 μA, which are two times higher. The Supplementary Fig. 4 shows the test results of alternately switching on and off the ground wire during the test of the TENG. It is observed that the output performance of this TENG is enhanced after grounding, the electrical signal returns to the original level after the second ungrounding, which adequately demonstrates the effectiveness of grounding strategy in analyzing the output signal of the TENG.

1.2. The mechanism of enhancing TENG's output performance using grounding strategy

Based on the above qualitative theoretical analysis, we preliminarily explained the enhancement mechanism of the grounding strategy on the TENG, and consider that the performance improvement comes from the inflow of electrons into the positive friction layer from the ground and the re-establishment of the dynamic equilibrium of electrons' gain and loss. Next, we will further study the enhancing mechanism of ground strategy in the next experiment. First, we designed a set of comparative experiments to clarify the enhancement effect. In the experiment, the three cases of comparison experiments have the same TENG structure but different wire connection mode. As shown in Fig. 2**a**, in structure, the upper part of the TENG consists of a Cu-paper-Cu structure, with the outer Cu as the electrode and the inner Cu as the positive friction layer; the lower part is a FEP-Cu double layer structure, with Cu as the electrode and FEP as the negative friction layer. In case I, only the positive friction layer is grounded, the open-circuit voltage and short-circuit current between this positive friction layer and the earth are measured. In case II, just like a normal TENG without connecting with ground, the load is connected between the upper electrode and the lower electrode. The open-circuit voltage and short-circuit current between them are tested by connecting these two electrodes. In case III, the positive friction layer is connected with the earth, and the load is connected between the upper electrode and the lower electrode, the open-circuit voltage and short-circuit current are tested between these two electrodes under grounding strategy condition. The test results are shown in Fig. 2**a**. The open-circuit voltage and short-circuit current of case III are up to 100 V and 1.0 μA, which are both two times higher than that of case II, which clearly shows the enhanced effect of the grounding strategy. Between the earth and the friction layer, we also tested the presence of 2 V open-circuit voltage and 0.03 μA short-circuit current respectively, they are alternating current pulses and the frequency is synchronized with the driving frequency. Although these signals are very weak, but they do prove the existence of electrons' flowing between ground and the positive friction layer, just as what we supposed in the working mechanism of grounding strategy. The working mechanism of GTNG and the charge transfer process are introduced in detail in Supplementary Note 2, and the schematic diagram is depicted in Supplementary Fig. 5**.** Next, on the basis of case III, two capacitors of 10 nF was separately added between the ground and the positive friction layer, and added between the upper and lower electrodes, to collect the flowing electrons between ground and positive friction layer and the flowing electrons between two electrodes. Fig. 2**b** depicts the test results of continuously collecting electrons for 1 h. It indicates that although the voltage at the two ends of the ground connected capacitor fluctuates periodically, the overall voltage curve still remains a slowly rising trend (without any rectifying circuit), which indicates that there is a one-way net inflow of electrons between ground and friction layer, that is to say, electrons do flow into the friction layer slowly from the ground. This is the direct evidence of the supposed working mechanism of enhancing effect of grounding strategy. On the other hand, we found that the capacitance voltage between the upper and lower electrodes of GTNG shows a slowly increasing trend with periodic fluctuations. This is also different from the normal TENGs. For a normal TENG, the whole system is closed, it is electrically neutral as a whole, so in the absence of rectification, its charge output for external system would be zero. However, after introducing the ground wire, the GTNG is connected with the earth, and the GTNG itself is no longer a closed system, so the GTNG is no longer electrically neutral of GTNG, which are 1.46 nC/min and 1.16 nC/min, respectively. In theory, they should be equal, we think the difference here is owing to the measurement error.

And, the schematic for the mechanism of net inflow of electrons is depicted in Supplementary Fig. 6**.** In fact, the current went through the grounding line is as alternating current signal, as shown in Fig. 2**b**. And the detail of the voltage waveform of the capacitor is shown in Supplementary Fig. 7. In stage 1, the positive and negative friction layers close contact with each other. The leaked electric field at the edge is very small. In stage 2, when the positive and negative friction layers separated, for the thicker dielectric layer, the electric field will be leaked at the edge (the Edge Effect). And the leaked electric field will drag extra electrons from the grounding wire into the positive layer. When the positive and negative friction layers contact again, in stage 3, some of the electrons, which flew into the positive layer in stage 2, will flow back into the ground. That is the source of generating alternating current signals in the grounding line. However, for the triboelectric effect, some electrons will transfer from positive layer into negative layer in stage 3. So, the surface charge density of the two fiction layers will increase and the leaked electric field will become larger than that in stage 1. The returning electrons are less than the inflow electrons. Therefore, there is net inflow of electrons between the positive triboelectric layer and the earth. Based on the theoretical research of TENG, it is concluded that the surface charge density increases with time and finally reaches saturation, this process is related to the speed of reaching maximum output of TENG. So, the charge accumulation process of GTNG without and with grounding strategy regulation is studied here. Fig. 2**d** represents the current curve in initial 30 mins' continuous working for the normal TENG without grounding, overall, it increases until reaching the maximum equilibrium value, but the increasing rate gradually decreases. We simply divide the process into three stages, k1, k2 and k3, depending on the rate of current increases. The average current growth rates of these three stages are 62, 18 and 6 nA/min, respectively. Fig. 2**e** shows the current curve for the case of GTNG with grounding. It also shows an overall increasing trend until reaching the maximum value, but in this curve, we can also find that its specific changing trend is significantly different from the current curve without grounding, and the linearity of current growth is more obvious. We divide the process into two stages, k1 and k2, depending on the increasing rate of the current. The average current growth rate of the two stages is 40 and 20 nA/min, respectively.

Also, we have analyzed the variation trend of CQC during charge accumulation before and after grounding strategy shown in

Supplementary Fig. 8 and f, the peak current value between normal TENG and GTNG shown in Supplementary Fig. 9, which comes to a consistent conclusion. Although the grounding strategy does not show advantages in the initial charge accumulation stage, the current growth rate of GTNG decreases more slowly with the increase of time, and the maximum output current at equilibrium state is much larger than that of the normal TENG without grounding. This further indicates that for GTNG utilizing the grounding strategy, the electrons in the ground will flow into the TENG, and the inflow of external charges will break the original equilibrium state inside the TENG, thus establishing a new charge equilibrium state with larger surface charge density and produce a higher output performance.

1.3. Further enhancing the output performance of GTNG through adding the dielectric layer

The effectiveness of the grounding strategy has been clarified by the above discussion. Then, a series of experiments will be conducted to analyze the influence of the dielectric layer on the output of GTNG with grounding strategy. When we took away the paper dielectric layer in the Cu-paper-Cu three-layer structure (upper part of GTNG), that is, the Cu layer plays the role of friction layer and electrode at the same time, just as shown in the schematic diagram of Supplementary Fig. 10. The positive friction layer is connected with ground and the lower electrode in the lower part of GTNG at the same time, when the layer becomes positively charged due to the loss of electrons [10], it will attract electrons from the earth and the lower electrode at the same time [40,41]. This will greatly reduce the enhancement effect of grounding strategy. Experimental test results are shown in the Supplementary Fig. 11. In this condition, the open-circuit voltage and short-circuit current of TENG increases from 3 5 V, 1 μA before grounding to 42 V, 1.2 μA after grounding, respectively. Although the enhancement effect still exists, but it is very weak.

Furthermore, the output performance of 14 groups of GTNG with different thickness of dielectric layers (0–70 μm) were tested. With the increase of dielectric layer thickness, the enhancement effect of grounding strategy gradually improved, and the short-circuit current under the same driving condition gradually increased from 1.2 μA to 3.1

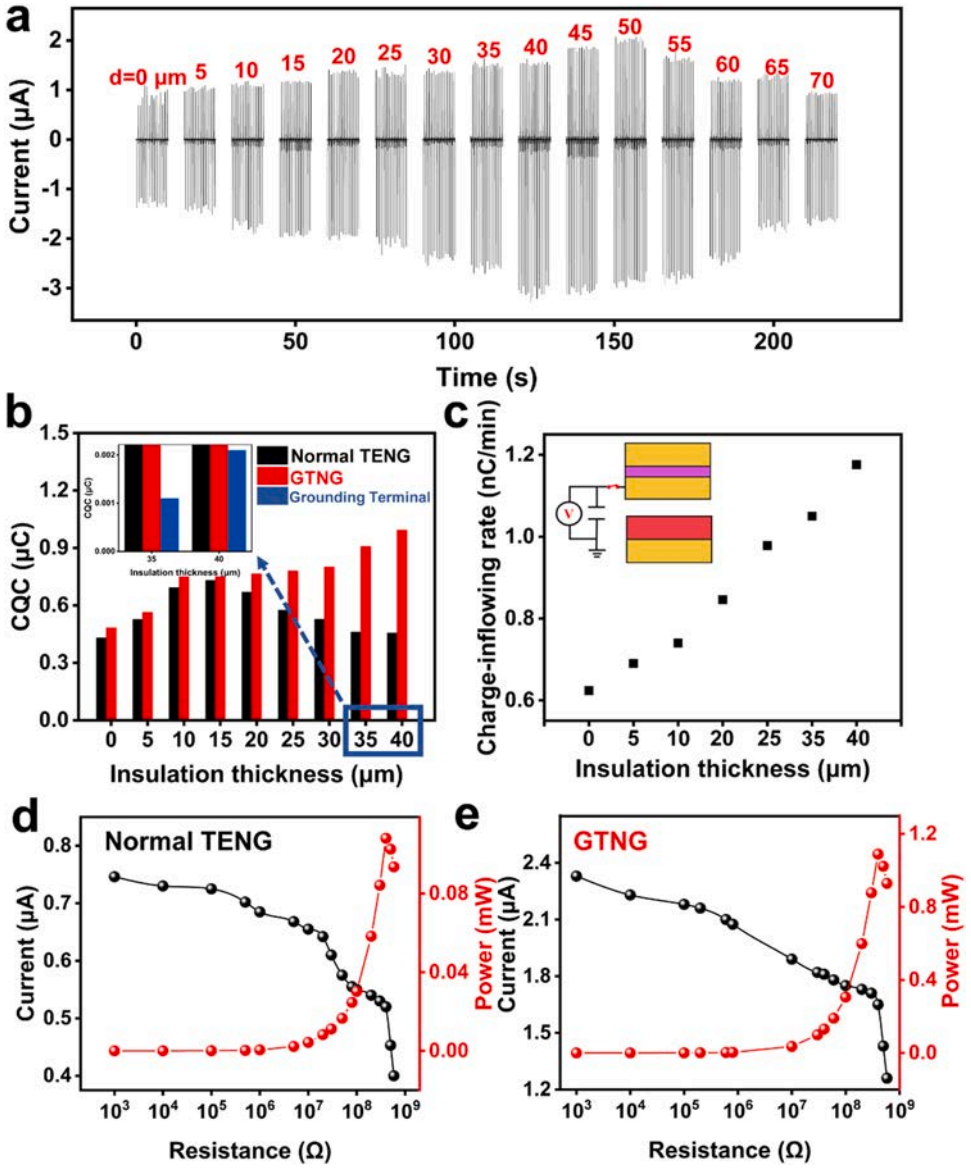

Fig. 3. (a) Current comparison of dielectric layers of different thicknesses of GTNG. (b) The CQC variation diagram of the dielectric layer with different thicknesses in three connection mode. (c) Comparison of charge-inflowing rate with different thickness dielectric layers. (d-e) Output current and power comparison of the normal TENG and the GTNG under different loads with the optimal dielectric thickness.

μA, the optimum thickness of dielectric layer is 45 μm as shown in Fig. 3**a**. And more detailed information such as the single-cycle voltage and current curves of GTNG with different dielectric thickness is shown in Supplementary Fig. 12. In order to make a clearer comparison, we calculated the charge quantity per cycle (CQC) of the TENG with different dielectric layer thicknesses (up to 40 μm) with (red column in Fig. 3b) and without grounding strategy (black column in Fig. 3b), the CQC flowing at the ground terminal (blue column in Fig. 3b). More detailed data can be seen in the Supplementary Fig. 13. It can be concluded that the CQC of TENG before grounding increases first and then decreases with the increase of dielectric layer thickness, which is consistent with the influence of friction layer thickness on normal TENG. But for GTNG, with the increase of dielectric layer thickness, the CQC monotonically increases with thickness in the whole range of test, and the maximum CQC reaches 1.0 μC. But the maximum CQC at the ground terminal is only 0.03 μC, which is extremely less compared with the output charge of the TENG. This small amount of charge is exactly from the electrons flowing from ground which causes the large improvement of GTNG's output. The electric field distribution under different dielectric thickness of GTNG is shown in Supplementary Fig. 14, that is the reason for the promotion of the dielectric layer on GTNG. In this figure, the positive friction layer lost some electrons and was positively charged. The upper electrode was negatively charged by the induced electrons. Ideally, when the thickness of dielectric layer goes to 0, the electric field between the positive friction layer and the upper electrode will be completely restricted in the plane-parallel capacitor. When the thickness of dielectric layer increases, the electric field will be leaked at the edge (the Edge Effect). And the leaked electric field will drag extra electrons from the grounding wire into the positive layer. The thicker the dielectric layer, the more leaked electric field and the more electrons will be introduced. These electrons can break the original balance of the triboelectric charges and increase the surface charge density of the friction layer.

On the other hand, the comparison of charge-inflowing rate with different dielectric layer thicknesses is researched in Fig. 3**c**, that the charge-inflowing rate increases with the increase of dielectric layer thickness. The inset in Fig. 3**c** shows the experimental circuit diagram, the electrons which collected in the capacitor are obtained from the earth. The detailed data diagram and the summarization is shown in the Supplementary Fig. 15**.** The optimal dielectric layer thickness based on this experimental model was obtained through these groups of comparative experiments.

Output power is one of the most important performance, so, next we explored the enhancement influence of grounding strategy on the output power of GTNG. Based on the above analysis of the dielectric layer, the output power is carried out using the optimal dielectric layer thickness of 40 μm. In the experiment, GTNG is composed of multilayer electrode structure, the output current and output power were tested for GTNG without and with grounding under different load conditions. As shown in Fig. 3**d and e**, the maximum power before grounding is 0.11 mW, and the maximum power after grounding is 1.1 mW, it is increased ten times through grounding. In addition, the durability test of GTNG has been conducted and shown in Supplementary Fig. 16, which presents high stability, and the output performance did not decrease after continuous work for 50 min. Through the above experiments, the effect of dielectric layer addition on the experimental model was clarified, and the working mechanism of the GTNG was shown in Supplementary Fig. 17. In the experiment, the optimal dielectric layer thickness for the experimental model was obtained, and the optimized conditions were adopted to test the output power, resulting in a ten-fold increase, which fully confirmed our above analysis and demonstrated the promotion effect of the addition of dielectric layer on the experimental model.

1.4. GTNG's output performance under different frequency and force and its potential in high-frequency energy harvesting

As for the experimental model itself, its own internal conditions have been optimized. Therefore, the composite electrode structure with the optimal dielectric layer thickness was selected for the subsequent experiments. The influence of driving frequency and driving force on the output performance of the grounding strategy will be explored in the following experiments. For a conventional TENG, the increase of driving force and driving frequency will improve the output performance of it. The former increases the friction charge separation rate by elevating the contact closeness of positive and negative friction layers. The latter improves the output performance of the TENG by magnifying the output cycle per unit time, and enables the TENG to reach to the equilibrium state faster. In general, changing the driving frequency only does not affect the separation rate of the friction charges and the charge bearing capacity of the friction layer in the stable state. However, in the grounding strategy, compared with the normal TENG, there is one more factor affecting the frictional charge carrying capacity, which is the net electron inflow from the earth to the positive friction layer linked by the grounding wire. As mentioned above, the inflow of these electrons can increase the maximum charge carrying capacity of the friction layer. The output performance diagram of case 1 shows the current in the grounding terminal which is an alternating current with the same frequency as the driving frequency (shown in Fig. 2**a**). Due to the asymmetry of positive and negative directions, a small amount of net inflow electrons will be injected into the surface of the positive friction layer in every cycle. In this way, compared with the traditional TENG, the increase of driving frequency can theoretically increase the electron injection rate from the grounding terminal to the positive friction layer, which will change the position of the dynamic charge equilibrium of the friction layer, that is, increase the charge carrying capacity of the friction layer under the same driving force. Therefore, 8 sets of controlled experiments were designed in this work to explore the influence of driving frequency and driving force on GTNG output.

Firstly, the driving frequency of the linear motor is changed while the external force remains still at 30 N. The output current of GTNG is shown in Fig. 4**a**, the short-circuit current increases with the increase of the driving frequency. In this figure, the enlarged detail can be found in Supplementary Fig. 18. Based on the measurement data in Fig. 4**a**, statistics are also made on the amount of charge quantity per cycle (CQC) at different frequencies, which is depicted in Fig. 4**b**. The data informs that in the process of each contact separation, the amount of electricity obtained in a single cycle will accelerate with the increase of frequency, showing a state of accelerated rise. As shown in Fig. 4**c**, when the driving frequency remains unchanged at 1.0 Hz and the external force on the GTNG is changed (the external force varies within the range of 5–160 N), based on these sets of data that when the driving frequency remains unchanged, the external force has a positive correlation with the GTNG model. Meanwhile, as depicted in Fig. 4**d**, we also analyzed the data of CQC driven by different external forces under this condition. This figure shows that in every contact separation process, the increase of external forces will contribute to the increase of CQC, and the growth rate will slow down with the increase of external forces, which is different from the influence of frequency on output performance. In order to observe the difference more clearly, the data of electrical signals has been collected under different forces and frequencies within a certain range. Fig. 4**e** depicts the overall comparison of the output current under different frequencies and forces using the grounding strategy. The horizontal coordinate is different driving force, and the lines in different colors in Fig. 4**e** represent different driving frequencies. The increase step of driving frequency is 5 Hz. From this figure, the influence of force on output current basically presents linear (of which color is black, red, blue, green and purple respectively) or decelerated growth (of which color is yellow). However, the influence of frequency on the output current presents an accelerated state, and the line spacing

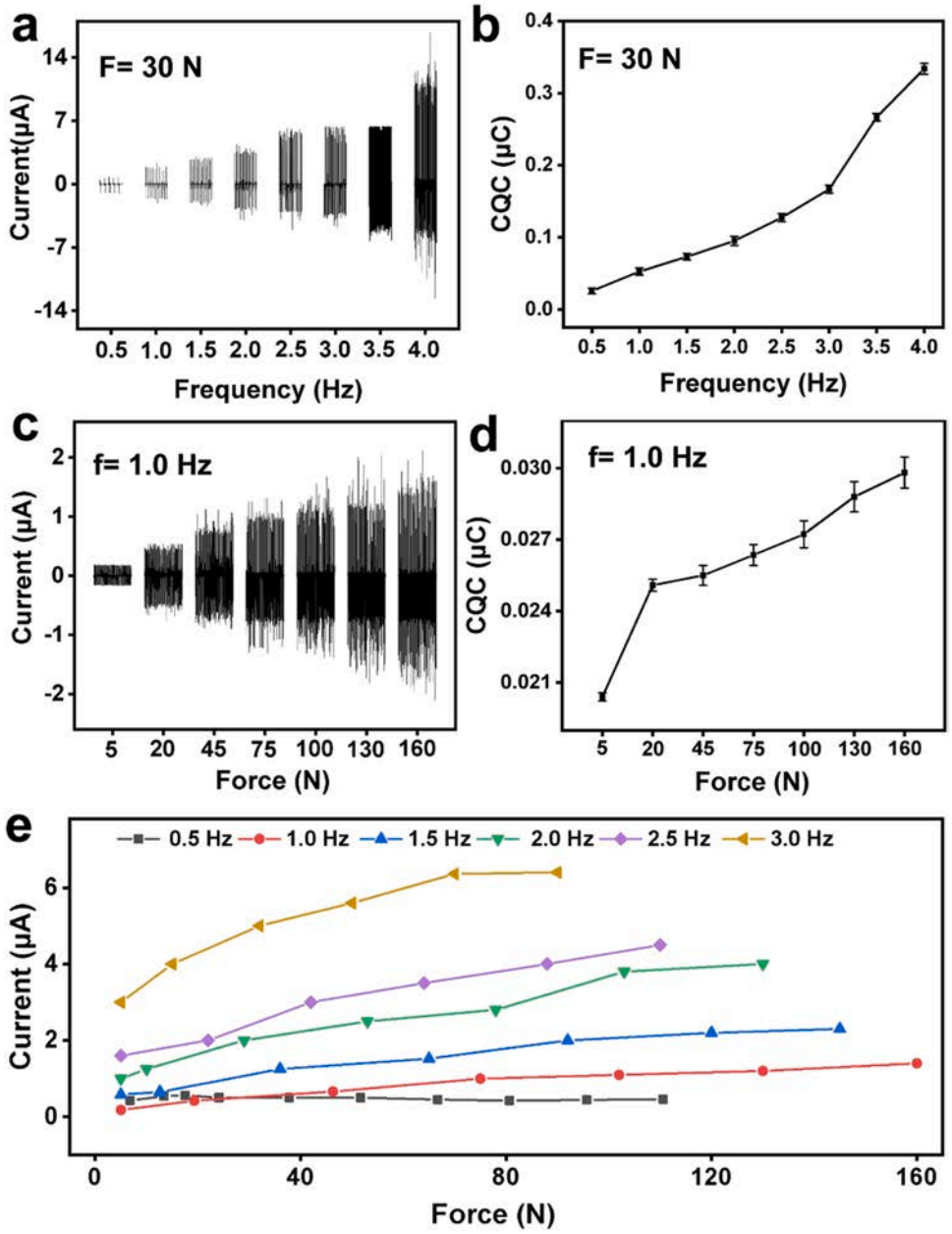

Fig. 4. (a,b) The current and the CQC comparison of GTNG at different frequencies and the same external force. (c,d) The current and CQC comparison of GTNG at different external forces and the same frequencies. (e) The current comparison of GTNG at different external forces and frequencies. (f) The charge-changing rate of external force and frequency of GTNG.

is increasing rapidly. So, the inference of the enhancement of driving frequency on GTNG which we mentioned above can be indirectly demonstrated. Therefore, we believe that the increase in driving frequency will bring more benefits to our grounding strategy. In other words, the GTNG scheme proposed by us is more suitable for some high-frequency energy collection scenarios, such as the collection and utilization of environmental sound wave energy. For this purpose, a ground strategy enhanced sound-wave driven triboelectric nanogenerator (GS-enhanced STNG) has been developed, the schematic diagram of the design is shown in Fig. 5**a**.

Structurally, the upper part of the GS-enhanced STNG is Cu-paper-Cu structure, with the outer layer of Cu as the electrode and the inner layer of Cu as the positive friction layer. The lower part is a FEP-Cu double-layer structure, with Cu as the electrode and FEP as the negative friction layer. In the experiment, the inner Cu electrode in the upper part of the structure is connected to the earth, and this device is placed at the Bluetooth speaker to provide sound source for GS-enhanced STNG. When the sound source is turned on, the sound wave will reach the surface of the device under the transmission of air vibration. Under the action of sound pressure, the FEP film will vibrate together with the vibration frequency of the sound wave, and the separated friction charge will generate electric potential at both ends of the electrode. This creates a flow of electrons in the outer circuit.

The influence of frequency and loudness on GS-enhanced STNG was studied. Firstly, the influence of frequency on the device was explored, as shown in Fig. 5**b**. When the loudness was kept constant at 70 decibels (in order not to cause noise pollution, appropriate loudness was selected here), we tested and compared the current values before and after using the grounding strategy, the statistics of charge quantity in the same time under this condition can be found in the Supplementary Fig. 19. Then based on the measurement, we define a calculation named the charge changing rate, by dividing the amount of charge per unit time after using

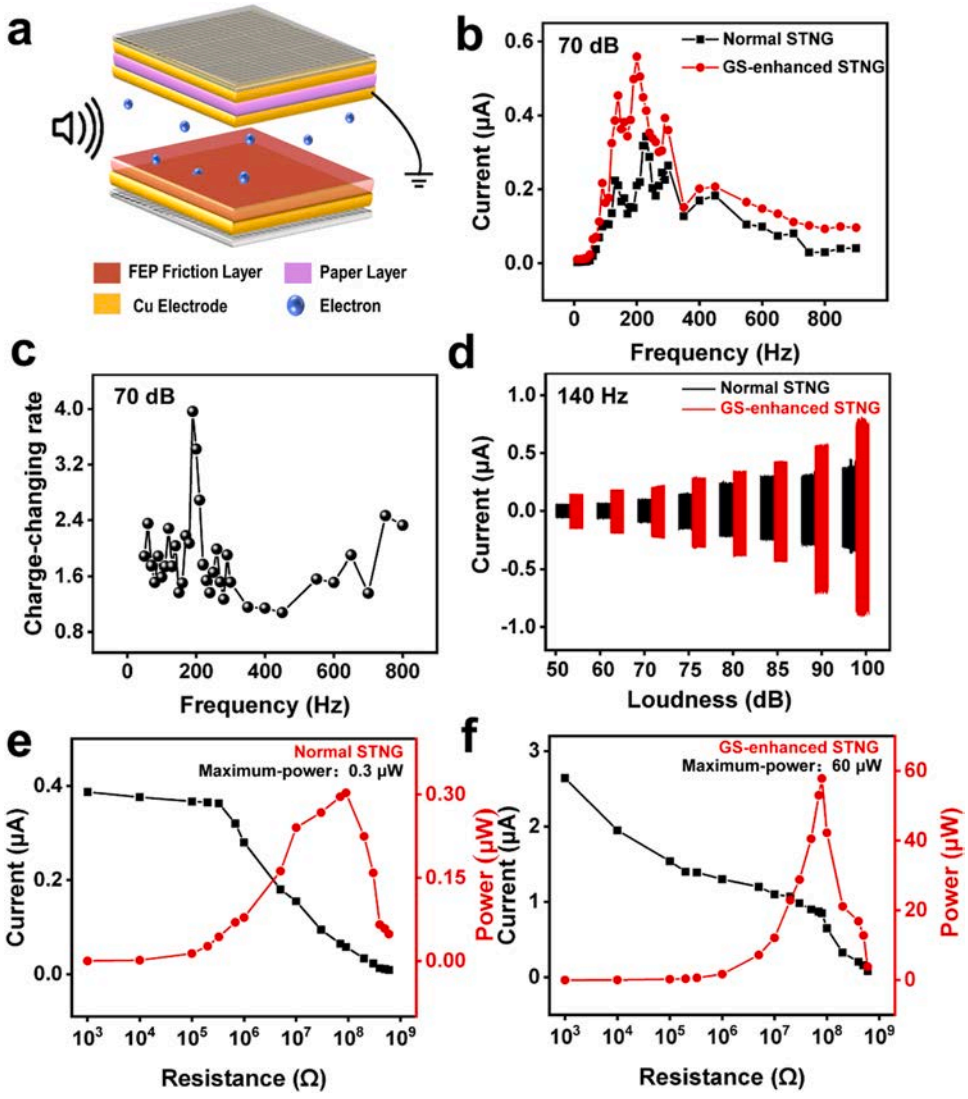

Fig. 5. (a) Schematic diagram of the GS-enhanced STNG structure. (b) Comparison of output current between the normal STNG and the GS-enhanced STNG at different frequencies when the loudness is 70 dB. (c) The charge-changing rate at different frequencies, when the loudness is 70 dB. (d) Comparison of output current between the normal STNG and the GS-enhanced STNG at different loudness when the frequency is 140 Hz. (e,f) Output current and power comparison between the normal STNG and the GS-enhanced STNG under different loads when the frequency is 140 Hz, the loudness is 70 dB.

grounding strategy by the amount of charge per unit time before using grounding strategy, as depicted in Fig. 3**c**, the charge changing rate is up to 4 times. When collecting electrical signals with different insulation thickness for GS-enhanced STNG, the optimization of insulation layer thickness for this model can make the charge changing rate up to 2 times (which is in the Supplementary Fig. 20). This contrast informs that frequency has a significant effect on the performance improvement of the GS-enhanced STNG output, and it verifies our previous conjecture. As shown in Fig. 5**d**, we keep the sound frequency unchanged at 140 Hz and only change the loudness. By comparing the current output before and after using grounding strategy, it can be seen that loudness also enhances the electrical signal.

Then, the same experimental conditions are remained to compare the output power before and after using the grounding strategy. Fig. 5**e and f** respectively show the current and power change curves under different loads when the loudness is 70 dB and the sound frequency is 190 Hz before and after using the grounding strategy, the statistics of charge quantity in the same time under this condition can be found in the Supplementary Fig. 21. The maximum power before using the grounding strategy is 0.3 μW and it reaches to 60 μW after using the grounding strategy, it increased by about 200 times. This result successfully confirms the theoretical analysis of the experimental model, which is suitable for energy collection at high frequency and can rapidly magnify the surface charge density to improve the output power. At the same time, the GS-enhanced STNG demonstrates a high sensitivity to high-frequency signals and external forces, and it is expected to have further development and application in the high-frequency energy-collection and self-driven sensing systems.

2. Conclusions

In conclusion, a charge supplement strategy for improving the output performance of TENGs is discovered and proposed in this paper. In this paper, a small number of electrons in the earth are extracted to promote the equilibrium movement of their own friction charge, thus more friction electrons are transferred from the positive friction layer to the negative friction layer. In this process, the maximum charge carrying capacity of the friction layer is increased to improve the overall output performance of TENG. The short-circuit current of the GTNG increases two times and the output power increases ten times. In addition, the effect in driven frequency can give GTNG a higher promotion in output performance compared to normal TENGs. Based on this characteristic, the STNG is designed, and the maximum output power is 0.3 μW without conducting the grounding strategy. By comparison, the maximum output power of GS-enhanced STNG is 60 μW, which was increased by about 200 times.

3. Methods and characterization

3.1. The preparation of GTNG

First, a composite electrode layer needs to be prepared, in which the upper layer Cu electrode and the middle layer Cu electrode have the same area of 25 cm^2. After attaching the upper layer Cu electrode to the base acrylic plate, the double-sided tape, which thickness is 5 μm, was utilized as the dielectric layer, and the thickness of the dielectric layer can be determined according to the number of layers of double-sided tape. The lower layer Cu electrode with the same area is pasted. Thus, the composite electrode layer is successfully prepared. Then prepare a 25 cm^2-FEP film and a 25 cm^2 lower layer Cu electrode, stick the lower layer Cu electrode on the base acrylic plate, and fix the FEP film on the lower layer Cu electrode. Then the GTNG required in this experiment has been prepared.

3.2. The preparation of GS-enhanced STNG

The GS-enhanced STNG is prepared by the same method as GTNG. However, the difference is that to make the sound waves act evenly on this device, the acrylic substrate is changed into a polyethylene film with uniform holes. Then the device is placed above the Bluetooth speaker to efficiently collect and convert the sound energy.

3.3. Characterization

A dielectric impedance analyzer (Novocontrol, BDS+50) was used to test the dielectric constant and dielectric loss in the experiment. The open-circuit voltage and short-circuit current of GTNG and GSS-TENG were tested by low noise preamplifiers SR 570 and SR 560, and Linear Motor (LinMot E1100) was applied to provide the driving force.

CRediT authorship contribution statement

Jingyi Jiao, Investigation, Methodology, Formal Analysis, Data curation, Writing - Original Draft, **Jinmei Liu,** Visualization, Investigation, **Long Gu,** Resources, Supervision, **Nuanyang Cui** Validation, Conceptualization, Project administration, writing original draft preparing, **Yong Qin,** Resources, Supervision, Funding Acquisition, Writing - Review & Editing.

Declaration of Competing Interest

The authors declare that they have no known competing financial interests or personal relationships that could have appeared to influence the work reported in this paper.

Data availability

Data will be made available on request.

Appendix A. Supporting information

Supplementary data associated with this article can be found in the online version at doi:10.1016/j.nanoen.2023.108310.

References

[1] X. Pu, M. Liu, X. Chen, J. Sun, C. Du, Y. Zhang, J. Zhai, W. Hu, Z.L. Wang, Sci. Adv. 3 (2017).
[2] Z.L. Wang, Acs Nano 7 (2013) 9533–9557.
[3] Z.L. Wang, J. Chen, L. Lin, Energy Environ. Sci. 8 (2015) 2250–2282.
[4] H. Yi, L. Xiong, J. Comput. Electron. 19 (2020) 1670–1677.
[5] B.K.Panigrahi Zeeshan, R. Ahmed, M.U. Mehmood, J.C. Park, Y. Kim, W. Chun, Appl. Energy 285 (2021).
[6] J. Ha, S.M. Kim, J.B. Kim, Integr. Ferroelectr. 183 (2017) 136–140.
[7] S.M. Kim, Eur. Phys. J. 133 (2018).
[8] C. Zhang, L. Zhou, P. Cheng, X. Yin, D. Liu, X. Li, H. Guo, Z.L. Wang, J. Wang, Appl. Mater. Today 18 (2020).
[9] L. Cheng, Q. Xu, Y. Zheng, X. Jia, Y. Qin, Nat. Commun. 9 (2018).
[10] S. Kim, J. Ha, J.-B. Kim, J. Comput. Electron. 15 (2016) 1593–1597.
[11] W. Liu, Z. Wang, G. Wang, G. Liu, J. Chen, X. Pu, Y. Xi, X. Wang, H. Guo, C. Hu, Z. L. Wang, Nat. Commun. 10 (2019).
[12] S. Wang, Y. Xie, S. Niu, L. Lin, C. Liu, Y.S. Zhou, Z.L. Wang, Adv. Mater. 26 (2014) 6720–6728.
[13] Y. Zi, C. Wu, W. Ding, Z.L. Wang, Adv. Funct. Mater. 27 (2017).
[14] Y. Zi, S. Niu, J. Wang, Z. Wen, W. Tang, Z.L. Wang, Nat. Commun. 6 (2015).
[15] J. Wang, C. Wu, Y. Dai, Z. Zhao, A. Wang, T. Zhang, Z.L. Wang, Nat. Commun. 8 (2017).
[16] X. Xia, J. Fu, Y. Zi, Nat. Commun. 10 (2019).
[17] X.-S. Zhang, M.-D. Han, R.-X. Wang, B. Meng, F.-Y. Zhu, X.-M. Sun, W. Hu, W. Wang, Z.-H. Li, H.-X. Zhang, Nano Energy 4 (2014) 123–131.
[18] C. Cai, B. Luo, Y. Liu, Q. Fu, T. Liu, S. Wang, S. Nie, Mater. Today 52 (2022) 299–326.
[19] R. Cao, X. Pu, X. Du, W. Yang, J. Wang, H. Guo, S. Zhao, Z. Yuan, C. Zhang, C. Li, Z. L. Wang, ACS Nano 12 (2018) 5190–5196.
[20] H. Zou, Y. Zhang, L. Guo, P. Wang, X. He, G. Dai, H. Zheng, C. Chen, A.C. Wang, C. Xu, Z.L. Wang, Nat. Commun. 10 (2019).
[21] H. Zou, L. Guo, H. Xue, Y. Zhang, X. Shen, X. Liu, P. Wang, X. He, G. Dai, P. Jiang, H. Zheng, B. Zhang, C. Xu, Z.L. Wang, Nat. Commun. 11 (2020).
[22] L. Shi, S. Dong, H. Xu, S. Huang, Q. Ye, S. Liu, T. Wu, J. Chen, S. Zhang, S. Li, X. Wang, H. Jin, J.M. Kim, J. Luo, Nano Energy 64 (2019).
[23] S. Wang, Y. Zi, Y.S. Zhou, S. Li, F. Fan, L. Lin, Z.L. Wang, J. Mater. Chem. A 4 (2016) 3728–3734.
[24] J. Fu, G. Xu, C. Li, X. Xia, D. Guan, J. Li, Z. Huang, Y. Zi, Adv. Sci. (Weinh) 7 (2020) 2001757.
[25] W. He, W. Liu, J. Chen, Z. Wang, Y. Liu, X. Pu, H. Yang, Q. Tang, H. Yang, H. Guo, C. Hu, Nat. Commun. 11 (2020) 4277.
[26] J. Wang, C. Wu, Y. Dai, Z. Zhao, A. Wang, T. Zhang, Z.L. Wang, Nat. Commun. 8 (2017) 88.
[27] K. Wang, J. Li, J. Li, C. Wu, S. Yi, Y. Liu, J. Luo, Nano Energy 87 (2021).
[28] K. Wang, C. Wu, H. Zhang, J. Li, J. Li, Nano Energy 99 (2022).
[29] J. Wu, Y. Xi, Y. Shi, Nano Energy 72 (2020).
[30] A. Šutka, K. Mālnieks, A. Linarts, M. Timusk, V. Jurķāns, I. Gorņevs, J. Blūms, A. Bērziņa, U. Joost, M. Knite, Energy Environ. Sci. 11 (2018) 1437–1443.
[31] Q. Tang, X. Pu, Q. Zeng, H. Yang, J. Li, Y. Wu, H. Guo, Z. Huang, C. Hu, Nano Energy 66 (2019).
[32] H.Y. Li, L. Su, S.Y. Kuang, C.F. Pan, G. Zhu, Z.L. Wang, Adv. Funct. Mater. 25 (2015) 5691–5697.
[33] W. Kim, T. Okada, H.-W. Park, J. Kim, S. Kim, S.-W. Kim, S. Samukawa, D. Choi, J. Mater. Chem. A 7 (2019) 25066–25077.
[34] L. Xu, T.Z. Bu, X.D. Yang, C. Zhang, Z.L. Wang, Nano Energy 49 (2018) 625–633.
[35] M. Tayyab, Z. Zhu, B. Wu, N.M. Abbasi, Y. Joseph, D. Gao, Energy Technol. (2022).
[36] H. Wu, S. Fu, W. He, C. Shan, J. Wang, Y. Du, S. Du, B. Li, C. Hu, Adv. Funct. Mater. 32 (2022).
[37] Y. Liu, W. Liu, Z. Wang, W. He, Q. Tang, Y. Xi, X. Wang, H. Guo, C. Hu, Nat. Commun. 11 (2020).
[38] Y. Bai, L. Xu, S. Lin, J. Luo, H. Qin, K. Han, Z.L. Wang, Adv. Energy Mater. 10 (2020).
[39] J. Chun, B.U. Ye, J.W. Lee, D. Choi, C.Y. Kang, S.W. Kim, Z.L. Wang, J.M. Baik, Nat. Commun. 7 (2016) 12985.
[40] N. Cui, C. Dai, J. Liu, L. Gu, R. Ge, T. Du, Z. Wang, Y. Qin, Energy Environ. Sci. 13 (2020) 2069–2076.
[41] J. Liu, N. Cui, T. Du, G. Li, S. Liu, Q. Xu, Z. Wang, L. Gu, Y. Qin, Nanoscale Adv. 2 (2020) 4482–4490.

Jiao Jingyi received her B.S from school of chemistry and materials science of Northwest University in 2018. She is currently a Ph.D. candidate in School of Advanced Materials and Nanotechnology, Xidian University, China. Her research interests mainly focus on the triboelectric nanogenerators and its enhancement mechanism.

Jinmei Liu received her B.S and Ph.D. from the School of Physical Science and Technology of Lanzhou University in 2011 and 2016, respectively. She is currently a lecturer in School of Advanced Materials and Nanotechnology, Xidian University, China. Her research focuses on the design and synthesis of new materials for energy harvesting devices, flexible self-powered system. She has abundant experiences on synthesizing inorganic oxide nanowire arrays and nanofbers, and fabricating flexible functional nanodevices.

Long Gu received his B.S and Ph.D. from the School of Physical Science and Technology of Lanzhou University in 2010 and 2016, respectively. He is currently a lecturer in School of Advanced Materials and Nanotechnology, Xidian University, China. From 2020.01–2022, he worked as a postdoctoral fellow in Professor Xudong Wang's group at University of Wisconsin-Madison. His current research focuses on piezoelectric and triboelectric nanogenerator, functional nanodevices, and self-powered systems.

Nuanyang Cui received his Ph.D. in Material Physics and Chemistry from Lanzhou University, China in 2015. He currently is an associate professor in School of Advanced Materials and Nanotechnology, Xidian University. His current research focuses mainly on the dynamic behavior of the triboelectric charges in the triboelectric nanogenerator (TENG) and the enhancement mechanism of TENG.

Yong Qin received his B.S. (1999) in Material Physics and Ph. D. (2004) in Material Physics and Chemistry from Lanzhou University. From 2007–2009, he worked as a visiting scholar and Postdoc in Professor Zhong Lin Wang's group at Georgia Institute of Technology. Currently, he is a professor at the Institute of Nanoscience and Nanotechnology, Lanzhou University, where he holds a Cheung Kong Chair Professorship. His research interests include nanoenergy technology, functional nanodevice and self-powered nanosystem. Details can be found at: http://www.yqin.lzu.edu.cn.